On the Optimal Teeth Geometry of a Hybrid Linear Stepper Motor

***SZABÓ LORÁND**, Ph.D.*
Technical University of Cluj
3400 CLUJ, P.O. Box 358., Romania
Tel.: (40)-(0)64-410-183, Fax: (40)-(0)64-192-055
e-mail: Lorand.Szabo@mae.utcluj.ro

Abstract: Hybrid linear stepper motors have been employed successfully in several industrial branches. As they operate under the variable reluctance principle the teeth geometries are very important. Therefore four teeth structures are taken into account to determine the optimum version. The field analysis in order to compute the electromagnetic forces of the motor is performed by using a computer package based on the finite element method.

1. Introduction

Hybrid linear stepper motors (HLSMs) are widely used in precise linear positioning systems because of their high speed, good positioning capability, ease of control and unlimited life expectancy [1].

The tangential thrust force is the most important performance parameter of the motor. It accelerates and decelerates the HLSM and drives the mover at predetermined speed while moving from one position to another. The normal force, as well the tangential force of the HLSM are strongly affected by the teeth configuration of the mover and platen. Therefore it is important to choose the best teeth geometry (the tooth pitch, tooth shape and the tooth width to tooth pitch ratio) in order to have a tangential force as great as possible and the smallest possible worthless normal attraction force. In this paper various teeth geometries are examined to determine the optimal one [2].

Because of the complex teeth geometry, salient pole structure and of the nonlinearities of the magnetic circuit a numerical method of solving the field problem is required. The finite element method (FEM) seems to be the best suited technique for these purposes.

Using a FEM computer package (MEZŐ, elaborated by the Electrical Drives and Machines Chair of the Technical University of Budapest) the different teeth configurations were compared. As results two force-displacement static characteristics of the tangential and of the normal force are presented. Two variants were selected as to be the best ones. For these variants the flux density variation in the air-gap was established. Taking into account also the manufacturing possibilities the optimum teeth geometry was selected for the HLSM.

2. The Hybrid Linear Stepper Motor

The HLSM consists of a mover that travels along a grooved steel platen (see Fig. 1).

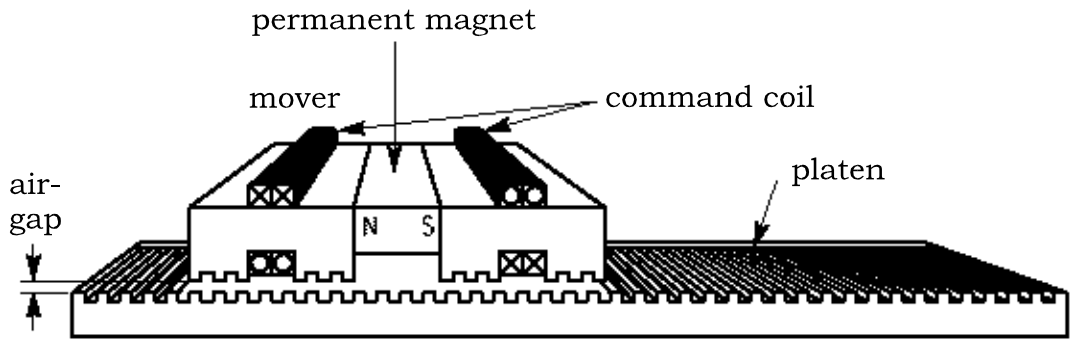

Figure 1. The hybrid linear stepper motor

The mover is composed of two electromagnets and a strong rare earth permanent magnet. The two pole faces of each electromagnet are toothed to concentrate the magnetic flux. The four sets of teeth on the mover are spaced in quadrature so that only one set at a time can be aligned with the platen teeth.

The motor works upon the combined operating principles of permanent magnet and variable reluctance motor types [3].

When current is established in a command coil, the resulting magnetic field tends to reinforce the permanent magnetic flux at one pole face and cancel it at the other. By reversing to phase the current, the reinforcement and cancellation are exchanged. By selectively applying current to the two command coils it is possible to concentrate flux at any of the mover's four pole faces. The pole receiving the highest flux concentration will attempt to align its teeth with the platen. Four steps result in motion of one tooth pitch [4].

The magnetic flux passing between the mover and the platen gives rise to a very strong normal attraction force between the two armatures. The attractive force can be up to 10 times the peak holding force of the motor, requiring a bearing arrangement to maintain precise clearance between the pole faces and platen teeth. Either mechanical roller bearings or air bearings are used to maintain the required clearance.

HLSM has the following benefits: low cost, ruggedness, simplicity in construction, high reliability, no maintenance, wide acceptance, no tweaking to stabilize, no feedback components are needed and it works in just about any environment. It is simple to drive and control in an open-loop configuration, too. A HLSM-driven positioning system is inherently stiff, with known limits to the dynamic position error.

3. Teeth Geometries

Four teeth configurations of the HLSM are considered (see Fig. 2). They cover adequately the most interesting cases.

In all the cases the air-gap length and the tooth pitch are the same:

$$g = 0.1\text{mm} \qquad \tau = 2\text{mm} \tag{1}$$

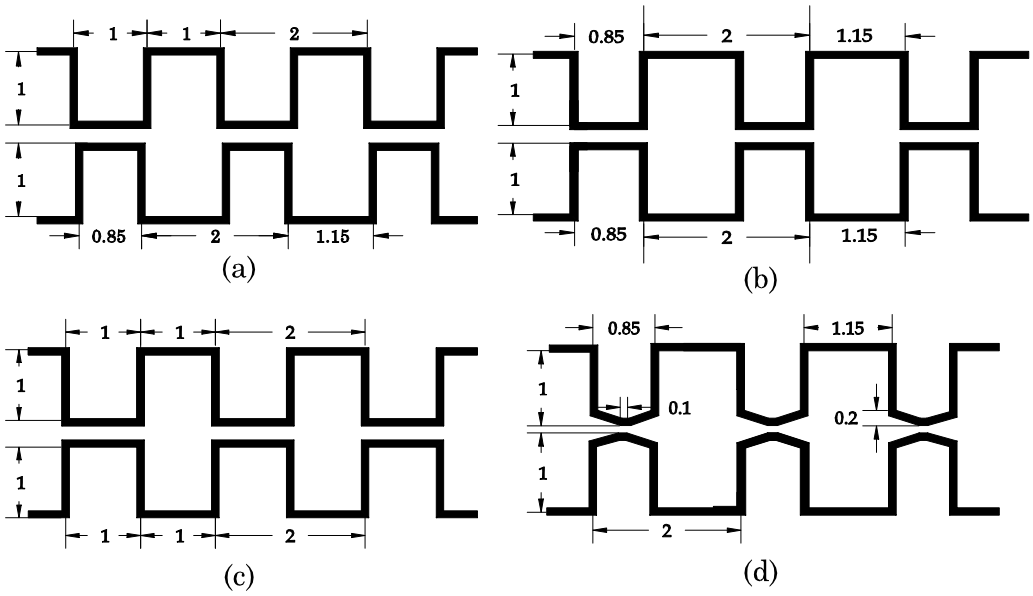

Figure 2. The considered teeth configurations of the HLSM

The first variant (Fig. 2/a) has different tooth width on the platen and on the mover, in order to concentrate the magnetic flux into the head of the platen teeth.

For the second version (Fig. 2/b) the tooth width is unequal to the slot width. As it was recommended in [5], the optimum tooth width to tooth pitch ratio is about *0.42*. So the widths of the tooth and of the slot are:

$$w_t = 0.85\text{mm} \qquad w_s = 1.15\text{mm} \tag{2}$$

The third teeth geometry (Fig. 2/c) is the "classical" one. The rectangle teeth on each side of the motor have the same width for the tooth and slot:

$$w_t = 1\text{mm} \qquad w_s = 1\text{mm} \tag{3}$$

The last air-gap structure in study is that having wedge headed teeth [6] and it is presented in Fig. 2/d. This structure has two more design parameters in addition to the tooth and slot width:

$$\theta_w = 20^{\text{o}} \qquad f_w = 0.1\text{mm} \tag{4}$$

whence θ_w 1 is the slop of the wedge and f_w 2 is the flat width at the wedge head.

4. Finite Elements Analysis

The finite elements magnetic field solution was used to determine the flux distribution and implicitly the electromagnetic forces of the HLSM.

The field model of the motor was obtained using the following assumptions [3]:

- The magnetic field quantities are independent of the *z*-coordinate. This leads to a two-dimensional analysis.
- Only the axially directed components of the magnetic vector potential and current density (A_z 3, respectively J_z 4) exist.
- The iron parts are isotropic and the corresponding nonlinear *B(H)*5 characteristics are single-valued (i.e. hysteresis effects are neglected).

- The anisotropic permanent magnet reveals an elemental magnetic orthotropy for the easy (*x*6) and difficult (*y*7) magnetization axes. Accordingly, the permanent magnet behavior in the easy *x*-axis being entirely explained in terms of demagnetization characteristic, *B(H)*8, and in the difficult *y*-axis being air-like.
- The external contour of the motor is treated as a line of zero vector potential, i.e. there is no field outside the motor periphery.
- Eddy-current effects are neglected.

From Hamilton's principle applied to macroscopic magnetostatics, the two-dimensional nonlinear variational field model of the HLSM involves the minimization, with homogeneous boundary conditions, of the following energy functional:

$$U(A_z) = \int_D \left[\int_0^{B_x} \nu_x \left(B_x - B_{r_x} \right) dB_x + \int_0^{B_y} \nu_y \left(B_y - B_{r_y} \right) dB_y - J_z A_z \right] dxdy \qquad (5)$$

where $\nu_x = f(B_x)$ 9, $\nu_y = f(B_y)$ 10 and B_{r_x} 11, respectively B_{r_y} 12 define the non-zero diagonal components of the reluctivity tensor and the remanent magnetic flux density, respectively, corresponding to the permanent magnet easy *x*-axis and difficult *y*-axis of magnetization. In the iron core portions $\nu = \nu(B)$ 13, $B_r = 0$ 14 and elsewhere in the considered domain *D*15, $\nu = \nu_0$ 16 and $B_r = 0$ 17.

By means of FEM the above energy-related functional is minimized by a set of trial functions, approximating the magnetic field solution. A usual FEM package has three main parts: pre-processing, processing and post-processing. Within the pre-processing sequence the next steps will be covered:

- The field domain *D*18 geometry is described and the subdomains are precisely defined.
- The boundary and the symmetry conditions are introduced.
- The field domain *D*19 is discretized into first-order triangular finite elements. Usually the packages have automatic mesh generators. In Fig. 3 the automatic generated mesh for the HLSM is shown.
- The material characteristics, *B(H)*20 curves, are selected from the package library or are defined for the subdomains.

The processing FEM sequence contains two phases: the global system generation and its iterative solution. All these are done automatically by the solver module.

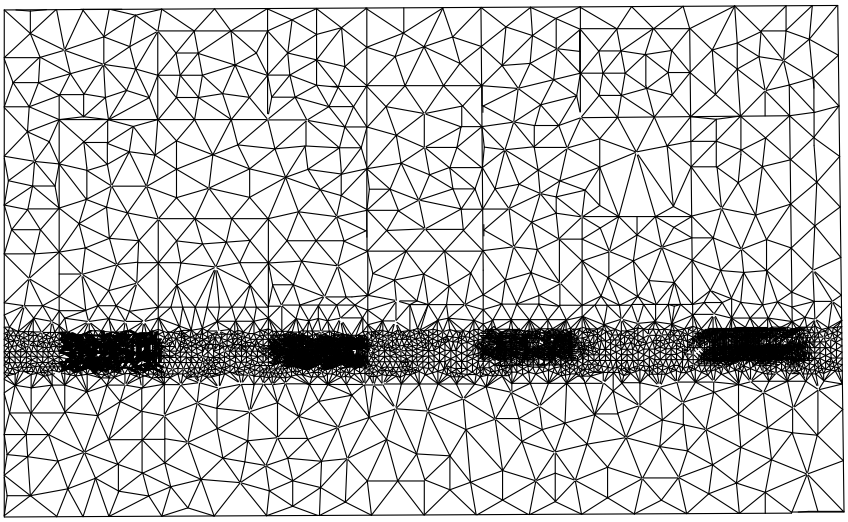

Figure 3. The discretized domain of the HLSM

In the post-processing part the obtained values of the magnetic vector potential at each mesh node are used to compute fluxes, magnetic energy, forces etc. All the packages have the possibility to show the magnetic flux distribution given by the magnetic potential constant lines.

In the post-processing FEM sequence the air-gap magnetic flux of each pole can be computed using the following line integral:

$$\Psi = \oint_{\Gamma} \overline{A} \overline{d}_{\Gamma} \tag{6}$$

The tangential force is computed by the surface integration of Maxwell's stress tensor:

$$f_t = \int_{\Sigma} \left[\nu_0 \left(\overline{B} \overline{n}_{\Sigma} \right) \overline{B} - \frac{1}{2} \nu_0 B^2 \overline{n}_{\Sigma} \right] d\Sigma \tag{7}$$

where the closed surface Σ 21 (having the unit outward vector normal $\overline{n}_{\Sigma}$ 22) surrounds the mover, passing through the centers of the air-gap mesh elements. The normal force is computed in a similar manner.

5. Results and Conclusions

Using the above mentioned FEM analysis package the force-displacement static characteristics of the tangential and of the normal force for the four considered teeth configurations were determined.

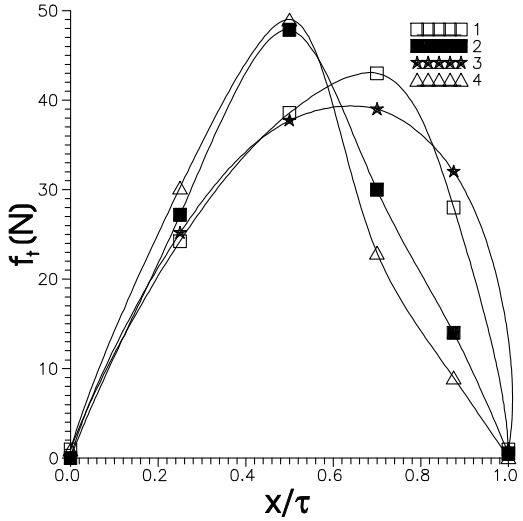

Figure 4. The tangential force vs. displacement static characteristics

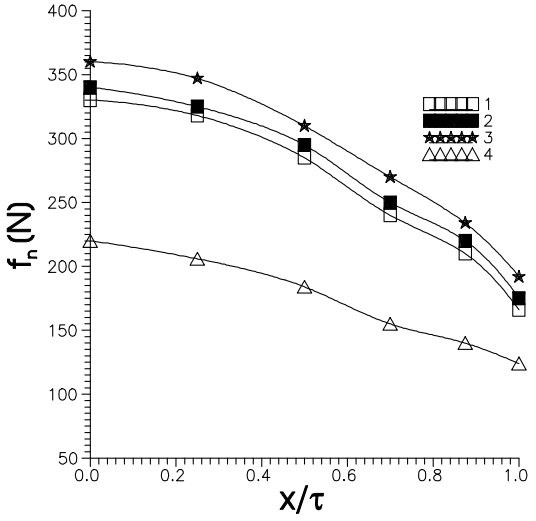

Figure 5. The normal force vs. displacement static characteristics

As it can be seen in Fig. 4, the total tangential force has its greatest peak value for the second and the fourth variant. The static characteristics of the total normal forces, presented in Fig. 5, show that the attraction force is reduced about to the half for the tooth structure having wedge head teeth. The other versions have almost the same normal force, but the second variant is smaller.

The optimal tooth geometry will be selected now from only two variants, the second and the fourth.

Next the plots of the flux densities in the air-gap under the poles will be studied. These figures were obtained from the above mentioned FEM analysis, too. Two situations were

considered: when the mover teeth are aligned with the platen teeth (Fig. 6) and when the teeth on both armatures are completely unaligned (Fig. 7). The continuous line corresponds to the fourth variant and the dashed line to the second one. As it can be seen from Fig. 7 the wedge heads of the teeth of the fourth variant are strongly saturated.

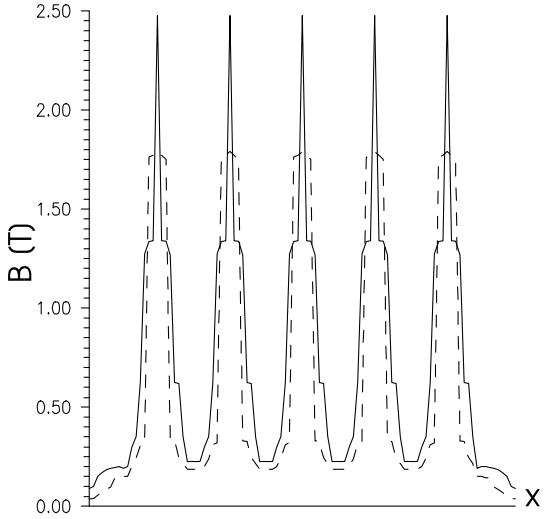

Figure 6. The flux density in the air-gap under an aligned pole

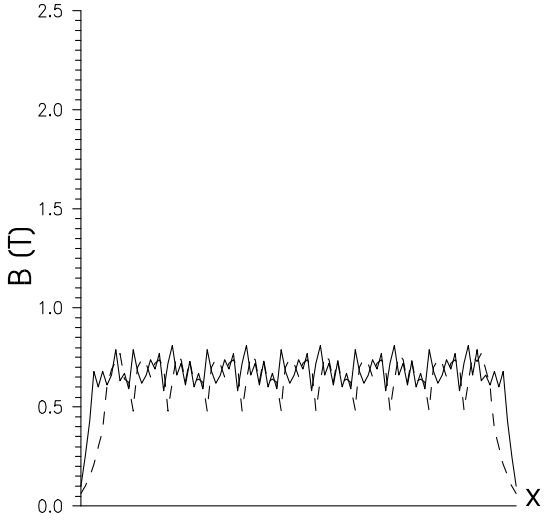

Figure 7. The flux density in the air-gap under an unaligned pole

Finally it can be concluded that the variant having wedge teeth has the greatest tangential force and far the less normal force. On the other hand is more difficult to manufacture this tooth construction than the other ones. Besides the heads of the teeth are very saturated in the aligned position of the teeth.

Therefore the use of the second variant is hardly recommended. It has almost as great tangential force as the fourth version in study, and its manufacture is more simple. In this case the shape of the tangential force-displacement static characteristic is near optimal, assuring high stiffness and therefore greater positional accuracy for the HLSM.

6. References

1. SZABÓ L. et al.: **Computer Simulation of a Constant Velocity Contouring System Using x-y Surface Motor**, Proceedings of the PCIM Conference, Nürnberg, 1995, Vol. Intelligent Motion, pp. 375-384.

2. BERTOLINI T.: **The Calculation of Stepper-Motors Torque in Regard to the Geometry of the Stator and Rotor-Teeth**, Proceedings of the International Conference on Electrical Machines , Pisa, 1988, pp.161-164.

3. VIOREL I.A. - SZABÓ L.: **Hybrid Linear Stepper Motors**, Mediamira Publishing House, Cluj-Napoca, Romania, 1998.

4. VIOREL I.A. - SZABÓ L.: **Permanent-magnet variable-reluctance linear motor control**, Electromotion, vol. 1., nr. 1. (1994), pp. 31-38.

5. KENJO T.: **Stepping Motors and their Microprocessor Controls**, Monographs in Electrical and Electronic Engineering, Vol. 16., Oxford Science Publications, 1985.

6. TAKEDA Y. et al.: **Optimum Tooth Design for Linear Pulse Motor**, Conference Record of the 1989 IEEE Industry Applications Society Annual Meeting, pp. 272-277.